

---

# RoMa: Revisiting Robust Losses for Dense Feature Matching

---

**Johan Edstedt**  
Linköping University

**Qiyu Sun**  
East China University of Science and Technology

**Georg Bökman**  
Chalmers University

**Mårten Wadenbäck**  
Linköping University

**Michael Felsberg**  
Linköping University

## Abstract

Dense feature matching is an important computer vision task that involves estimating all correspondences between two images of a 3D scene. In this paper, we revisit robust losses for matching from a Markov chain perspective, yielding theoretical insights and large gains in performance. We begin by constructing a unifying formulation of matching as a Markov chain, based on which we identify two key stages which we argue should be decoupled for matching. The first is the coarse stage, where the estimated result needs to be globally consistent. The second is the refinement stage, where the model needs precise localization capabilities. Inspired by the insight that these stages concern distinct issues, we propose a coarse matcher following the regression-by-classification paradigm that provides excellent globally consistent, albeit not exactly localized, matches. This is followed by a local feature refinement stage using well-motivated robust regression losses, yielding extremely precise matches. Our proposed approach, which we call RoMa, achieves significant improvements compared to the state-of-the-art. Code is available at <https://github.com/Parskatt/RoMa>

## 1 Introduction

Feature matching is the computer vision task with the goal of finding pixel-pairs corresponding to the same 3D point from two images, and is crucial for downstream tasks such as 3D reconstruction [43]. The recently popularized dense feature matching paradigm [54, 26, 57, 14] aims to find all matching pixel-pairs between the images. These methods employ a coarse-to-fine approach, whereby dense matches are first predicted at a coarse level and successively refined at finer resolutions.

While these methods empirically work well, there is a lack of a theoretical framework to analyze modeling choices, such as architecture and loss formulation, which are critical for performance. For example, recent methods typically use the same loss function for both coarse matching and refinement, coupling the tasks of matching and refinement together. Furthermore, they use simple regression losses during training despite the fact that feature matching is prone to outliers [52, 53, 2]. However, without a theoretical foundation, analyzing the consequences of these choices is difficult.

To solve this issue we propose a unifying probabilistic framework, where we model matching as a non-stationary diffusion process [64, 45, 23, 46] using a Markov chain formulation. In this framework, we identify two key stages, the coarse matching stage, and the refinement stage (see Figure 1). In the first stage, complex free-form distributions should be modeled in order to account for the impact of motion boundaries and repeating structures in the scene. In this stage, global consistency is critical, in order to initialize the refinement in the correct basin of convergence. However, exact localization is of lesser importance, as the refinement stage can be relied on to converge to the local optimum.

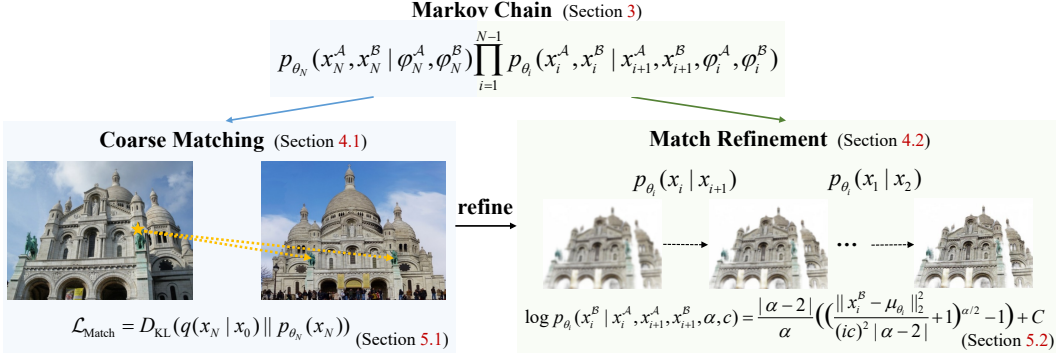


Figure 1: **Illustration of our approach RoMa.** We cast matching in a Markov chain probabilistic regression framework. In this framework we are able to analyze matching from a novel perspective, see Section 3. First, we argue from a scale-space perspective that matching and refinement should be decoupled, which we explore further in Section 4. Second, we revisit the typical refinement loss formulation from the Markov perspective, comparing it to alternative autoregressive formulations. Motivated by our insights we propose a set of robust losses, see Section 5.

In the second stage, in contrast, we can model the conditional as a unimodal Gaussian with a small variance, given that the coarse prediction is approximately correct. Here global consistency is of little importance, and precise localization is key. See Section 3 for details.

Motivated by the theoretical insight that the coarse matching and refinement stages should be seen as decoupled tasks, requiring different sets of features and architectures, we split the learning of the coarse matcher and refinement. We propose specialized networks for each task, focusing on a locality-free globally consistent architecture for coarse matches combined with precise local features for refinement. See Section 4 for details.

While refinement can be modeled as Gaussian for approximately correct matches, if the conditioning from previous steps is poor the model receives spurious gradients from outliers. An alternative approach is to directly condition on the forward process  $q$ . This alternative eliminates the outlier problem. However, as discussed in Section 3, this approach faces challenges with distribution shifts during inference. Hence, it is interesting to explore how to interpolate between these two extremes. We do this by robust regression losses, which is further discussed in Section 5. In this way we can mitigate the adverse consequences caused by outliers, promoting better gradient propagation training and thus achieving more accurate matching results.

Our full approach, which we call RoMa, is illustrated in Figure 1. We qualitatively compare matching results of RoMa to the state-of-the-art method DKM [14] in Figure 2.

In summary, our contributions are as follows:

- (a) We propose a Markov chain theoretical framework for dense matching. See Section 3.
- (b) We decouple the coarse matching and refinement stages. We propose a globally consistent approach for coarse matches and precise local features for refinement. See Section 4.
- (c) Finally, we revisit robust losses. We propose *regression by classification* for coarse matching followed by robust regression losses for refinement. See Section 5.
- (d) We conduct an ablation study, and SotA experiments on competitive benchmarks. We find that the proposed decoupling and robust losses yield improvements. See Section 6.

## 2 Related Work

### 2.1 Sparse → Detector Free → Dense Matching

Feature matching has traditionally been approached by keypoint detection and description followed by matching the descriptors [33, 4, 12, 40, 41, 58]. Recently, the detector-free approach [48, 7, 50, 10] replaces the keypoint detection with dense matching on a coarse scale, followed by mutual nearest



Figure 2: **Qualitative comparison.** The SotA method DKM [14] (left) compared to RoMa (right).

neighbors extraction, which is followed by refinement. The dense approach [35, 55, 56, 14, 67, 37] instead estimates a dense warp, aiming to estimate every matchable pixel pair.

## 2.2 Markov Chains, Robust Regression Losses, Regression by Classification:

**Markov Chains and Diffusion:** Diffusion models [45, 23] cast image generation as learning the reverse process of a known forward process. This objective has many similarities to score matching and denoising autoencoders [25, 59, 46, 47, 27]. In this work, we additionally connect scale-space [64, 28, 30] diffusion to our Markov chain formulation. In contrast to recent generative work, our modeled forward process does not converge to a parameter-free distribution (see Section 3). This motivates our proposed decoupled learning of coarse matching and refinement (see Section 4).

**Robust Regression Losses:** Robust loss functions provide a continuous transition between an inlier distribution (typically highly concentrated), and an outlier distribution (wide and flat). Robust losses have, e.g., been used as regularizers for optical flow [5, 6], robust smoothing [15], and as loss functions [3, 32].

**Regression by Classification:** Regression by classification [62, 63, 51] involves casting regression problems as classification by, e.g., binning. This is particularly useful for regression problems with sharp borders in motion, such as stereo disparity [16, 20]. Closest to our work, Truong et al. [57] propose a mixture model for self-supervised dense matching, aiming to let the model predict non-matchable pixels.

**Classification then Regression:** A classical approach to classification-then-regression is classification-regression decision trees [8, 39]. Closer to our work, Li et al. [29], and Budvytis et al. [9] proposed hierarchical classification-regression frameworks for visual localization. LoFTR [48] optimize the model log-likelihood of mutual nearest neighbors, followed by  $L_2$  regression-based refinement. In contrast, we aim to estimate the full matching distribution, i.e., dense feature matching. We propose a theoretical framework to analyze modeling choices, and revisit robust regression.

## 3 Dense Matching as a Markov Chain

Dense feature matching is, given two images  $I^A, I^B$ , to estimate a dense warp  $W^{A \rightarrow B}$  (mapping coordinates  $x^A$  from  $I^A$  to  $x^B$  in  $I^B$ ), and a matchability score  $m^{A \rightarrow B}$  for each pixel. From a probabilistic perspective,  $p(W^{A \rightarrow B}) = p(x^B | x^A)$  is the conditional matching distribution, while  $m$  is the marginal distribution  $p(x^A)$ . Multiplying these yields the joint distribution. The end goal is to obtain a good estimate of the probability distribution over correspondences of coordinates  $x^A$  in image  $I^A$  and coordinates  $x^B$  in image  $I^B$ . Obtaining this would mean that we know which coordinates in  $I^A$  are likely to match with which coordinates in  $I^B$ .

We explicitly model the match probabilities as a Markov chain in the following way,

$$p_{\theta}(x^A, x^B | I^A, I^B) = p_{\theta_N}(x_N^A, x_N^B | \varphi_N^A, \varphi_N^B) \prod_{i=1}^{N-1} p_{\theta_i}(x_i^A, x_i^B | x_{i+1}^A, x_{i+1}^B, \varphi_i^A, \varphi_i^B), \quad (1)$$

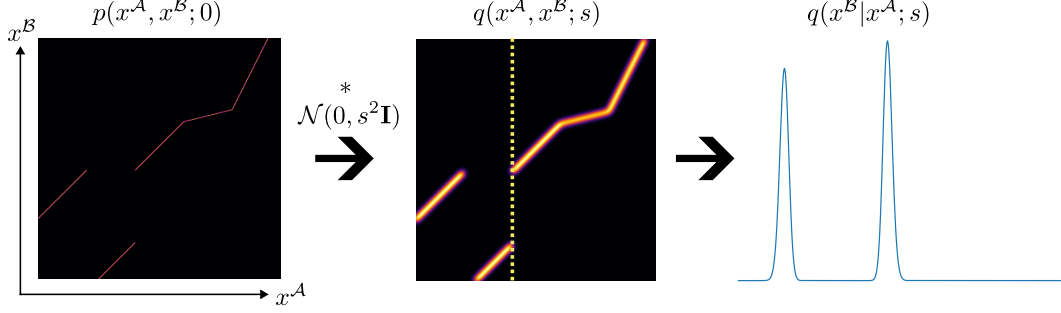


Figure 3: **Illustration of localizability of matches.** We illustrate the uncertainty in the joint match distribution at some scale  $s$ , corresponding to the forward Markov process  $q$ . Note the multimodality in the conditional distribution  $q(x^B|x^A; s)$  due to motion boundaries.

where the  $\{i\}$  indicates scale, the finest being 1 and the coarsest  $N$ ,  $\theta$  is a set of trainable parameters, and  $\varphi_i = E_{\theta_i}(I)$  are features extracted by encoders  $E_{\theta_i}$  from the images. In what follows, we assume the condition on  $\varphi$  to be fulfilled and omit the condition to reduce notational clutter. The way to interpret Equation (1) is that we first have a coarse matching problem of estimating  $p_{\theta_N}$  given only some coarsely extracted features and then we have a chain of refinement matching problems where we estimate  $p_{\theta_i}$  given the estimated matches at the coarser scale  $i + 1$ . We will discuss the decoupling into two different types of matching problems in detail in Section 4. Note that the transition functions  $p_{\theta_i}$  are *not* stationary, i.e., their parameters will depend on the scale.

While it is straightforward to cast matching models as a Markov chain, it is less clear how to design a suitable loss. One possible way to do this is to optimize a variational lower bound, as in diffusion models [45, 23], which optimize

$$\mathbb{E}[-\log p_{\theta}(x_0)] \leq \mathbb{E}_q \left[ D_{\text{KL}}(q(x_N|x_0)||p_{\theta_N}(x_N)) + \sum_{i=1}^{N-1} D_{\text{KL}}(q(x_{i-1}|x_i, x_0)||p_{\theta}(x_{i-1}|x_i)) + p_{\theta_1}(x_0|x_1) \right], \quad (2)$$

where we defined  $x_i = (x_i^A, x_i^B)$  for notation compactness. Having the model reverse a forward process  $q$  has proved very successful. However, this requires a reasonable definition of what a forward process ought to be for matching.

### 3.1 A Forward Chain for Matching

We will utilize scale-space theory [64, 28, 30] to define a plausible forward process for matching. The image scale-space is parameterized by a parameter  $s$ ,

$$L(x, s) = \int g(x - y; s) I(y) dy, \quad (3)$$

where

$$g(x; s) = \frac{1}{2\pi s^2} \exp\left(-\frac{1}{2s^2} \|x\|^2\right) \quad (4)$$

is a Gaussian kernel. Motivated by this, we define the *localizability* of matches as

$$q(x^A, x^B; s) = \mathcal{N}(0, s^2 \mathbf{I}) * p(x^A, x^B; 0), \quad (5)$$

where the infinite resolution  $p(x^A, x^B; 0)$  can be represented as a set of impulse functions  $\delta$ , and  $s = ic$  for some  $c \in \mathbb{R}^+$ . Our model, while simple, provides an explanation for multimodal matches at motion boundaries. For large scales, features increasingly mix, leading to the conditional  $q(x^B|x^A; s)$  becoming multimodal. We illustrate the process qualitatively in Figure 3. Note that, besides this aleatoric uncertainty, repeating structures are common in real-world scenes (as shown in Figure 1), indicating an even larger need for multimodal prediction.

### 3.2 Analysis of Coarse Matching

**Properties of a Suitable Coarse Matcher:** Revisiting Figure 3, it is important to note that large regions of the match space has low density due to the fact that  $p$  is a lower dimensional manifold. This has the implication that it is critical for the coarse matcher to be *globally* consistent, but *local* precision is unimportant as once in a high density area we can expect the refinement to converge to the local maximum. Reciprocally, if the coarse matching provides a globally incorrect initialization the refinement stage is unlikely to recover, no matter how locally precise the matcher is. Based on these observations, we propose an improved coarse matcher in Section 4.1.

**Coarse Matching Loss:** Given the forward process, we can define a coarse matching loss

$$D_{\text{KL}}(q(x_N|x_0)||p_{\theta_N}(x_N)). \quad (6)$$

A typical choice of  $p_{\theta_N}(x_N)$  would be a Gaussian with a standard deviation equal to  $s$ . However, as we illustrated in Figure 3, the distribution is multimodal. This is particularly troublesome at motion boundaries and for repeating structures. Motivated by this, we propose to model the coarse matching stage distribution in a free-form way by regression by classification. We describe this in more detail in Section 5.1.

### 3.3 Analysis of Refinement

**Properties of Suitable Refiners:** Again revisiting Figure 3, we will assume that the coarse matching stage provides the refinement stage with generally globally consistent, albeit perhaps imprecise, initialization. If that is the case, there is no need for the refiner to be globally consistent. Instead, it is of much greater importance that the model be able to *locally* precisely refine. Comparing this to the coarse matcher, it is noticeable that the desired properties are reversed. This motivates a *decoupled* formulation of coarse matching and refinement. We further develop this argument in Section 4.2.

**Refinement Loss:** Interestingly, refinement losses [55, 14] for dense feature matching do not optimize an autoregressive objective as in Equation (2), but rather condition on the model predictions themselves. In our probabilistic framework, we can formulate such refinement losses as

$$\sum_{i=1}^{N-1} \mathbb{E}_{x_{i+1} \sim p_{\theta_{i+1}}} \mathbb{E}_{x_i \sim q(x_i|x_0)} [-\log p_{\theta_i}(x_i|x_{i+1})]. \quad (7)$$

Under the assumption that  $p_{\theta_i}$  is Gaussian with variance equal to  $q(x_i|x_0)$ , and that  $q(x_i|x_0) = \mathcal{N}(x_i; x_0, s^2\mathbf{I})$ , where  $s = ic$  for some constant  $c$ , this can be rewritten as

$$\sum_{i=1}^{N-1} \mathbb{E}_{x_{i+1} \sim p_{\theta_{i+1}}} \left[ \frac{1}{2s^2} \|\mu_{\theta_i}(x_{i+1}) - x_0\|_2^2 \right]. \quad (8)$$

While this intuitively seems reasonable, it is problematic when the conditioning for the refinement is wrong, as we illustrate in Figure 4. Another approach is to optimize an autoregressive variational bound as in diffusion models, given by

$$\mathbb{E}[-\log p_{\theta}(x_0)] \leq \mathbb{E}_q \left[ D_{\text{KL}}(q(x_N|x_0)||p_{\theta_N}(x_N)) + \sum_{i=1}^{N-1} D_{\text{KL}}(q(x_{i-1}|x_i, x_0)||p_{\theta}(x_{i-1}|x_i)) + p_{\theta_1}(x_0|x_1) \right]. \quad (9)$$

A simplified version

$$\mathbb{E}_{i, x_0, x_i} [\|x_0 - \mu_{\theta_i}(x_i)\|^2] \quad (10)$$

is often used [59, 23, 47, 27] in practice, where  $p_{\theta_i}$  is assumed to be Gaussian and the weighting is removed. However, as we illustrate in Figure 4, distribution shifts between the forward and reverse process make autoregressive variational objectives problematic during inference.

### 3.4 Observations

Motivated by our analysis we make two key observations:

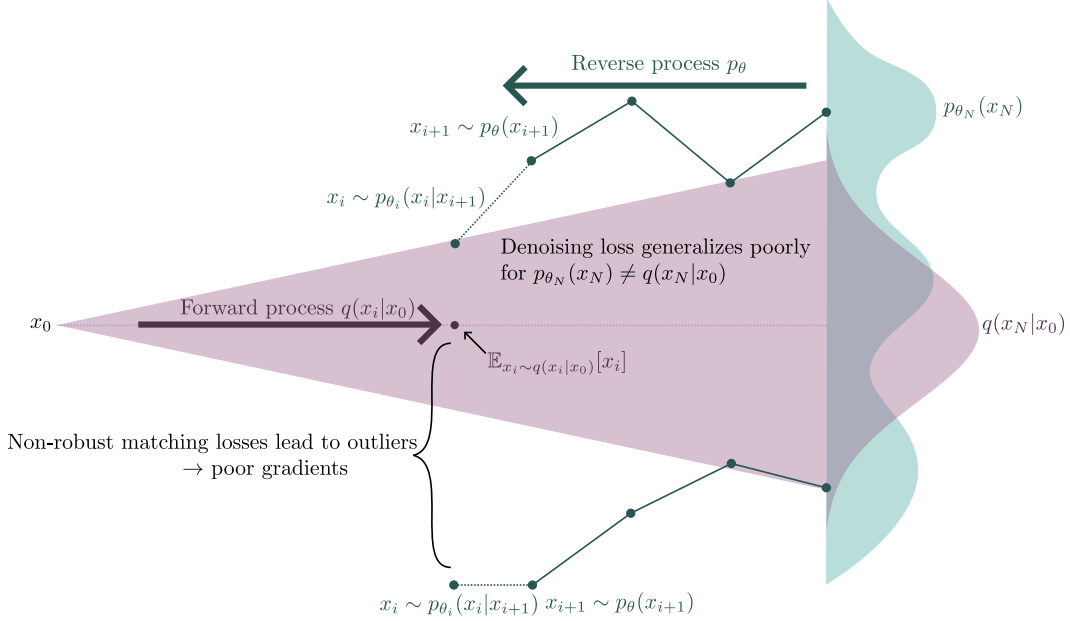


Figure 4: **Illustration of issues with current refinement losses.** Denoising objectives generalize poorly in cases where  $p_{\theta_N}(x_N) \neq q(x_N|x_0)$ , as it leads to out-of-distribution conditioning for the refinement. However, typical non-robust matching losses (which condition on model predictions) create outliers, and yield poor gradients. Hence, a more ideal loss would be somewhere in between, we propose such a loss in Section 5.

- Coarse matching fundamentally differs from refinement, due to the desired properties of the matcher being reversed (global consistency vs precise localizability). We hence propose to decouple them. In Section 4 we discuss how to achieve this.
- Given the decoupled stages, we are left with choosing appropriate loss functions. We argue for the regression-by-classification formulation for coarse matching and for robust regression losses for refinement in Section 5.

## 4 Decoupling Coarse Matching and Refinement

Given that coarse matching and refinement benefit from different properties, we ask the following:

*Can we improve matching by using separate networks for the coarse matching and refinement stage?*

The answer, as we empirically demonstrate in Section 6.3, is yes.

We will now describe our network choices for the two stages. By *encoders* we mean the networks  $E_{\theta_i}$  that operate on the input images and output the features  $\varphi_i$  that we condition the matching on in Equation (1). By *decoders* we mean the networks that estimate the warp.

### 4.1 Coarse Matching

**Coarse Encoder:** Previous dense work [57, 14] use CNN encoders. However, transformer-based models have been shown to have better global consistency. In particular, they are more robust to natural perturbations [36], and exhibit a higher shape bias [18] which is needed for a consistent coarse matcher. We choose the recent ViT [13] based unsupervised model DINOv2 [38] as the coarse encoder. DINOv2 provides several advantages for feature matching compared to previous models. Firstly, the high-resolution pretraining takes advantage of frozen features, without fine-tuning, which makes training significantly faster. Secondly, unsupervised pretraining typically correlates better with non-semantic tasks than supervised counterparts [61, 22, 38].

**Coarse Decoder:** In initial experiments, we found that CNN-based coarse match decoders overfit to the training resolution. Additionally, they tend to be over-reliant on locality. While locality is a powerful cue for refinement, it leads to oversmoothing for the coarse warp. To address this, we propose a *position encoding free* transformer decoder. By restricting the model to only propagate by feature similarity, we found that the model generalized significantly better. The proposed architecture is detailed in the appendix.

## 4.2 Refinement

**Local Feature Encoder:** For the refinement stage, we found it sufficient to improve the encoder. Previous work [31, 42, 21, 57] indicates that VGG19 [44] features are more precisely localizable than ResNet features. Furthermore, they exhibit a strong texture bias [17]<sup>1</sup>, which we argue is actually an advantage for localizability. More recent work [14, 67] however, still uses ResNet features. This is likely due to the confounding coupling effect, whereby highly localizable features tend to produce worse global consistency. We find that when using decoupled learning, VGG19 local features outperform ResNet local features.

## 5 Robust Losses for Matching

Motivated by the insights in Section 3, we now propose an improved loss formulation for matching.

### 5.1 Coarse Matching Loss

Previous work typically models the coarsest warp  $W_N$  as unimodal [55, 14],

$$\log p_\theta(x_N^B | x_N^A) \propto \|x_N^B - \mu_{\theta_N}\|_2^p. \quad (11)$$

However, as is illustrated in Figure 3, unimodal distributions cannot represent matching distributions at motion boundaries (due to Aleatoric uncertainty) and for repeating structures (due to Epistemic uncertainty). Motivated by this, we will instead let the model predict a free-form discretized distribution. To do this, we will consider the *regression by classification* formulation, whereby we discretize the output space. We choose the following formulation,

$$p_{\theta_N}(W_N) = \sum_{k=1}^K \pi_k \mathcal{B}_{\mu_k}, \quad (12)$$

where  $K$  is the quantization level,  $\pi_k$  are the probabilities for each component,  $\mathcal{B}$  is some 2D base distribution, and  $\{\mu_k\}_1^K$  are anchors. Assuming non-overlapping bins and that  $\mathcal{B} = \mathcal{U}$ , the Kullback–Leibler divergence is

$$D_{\text{KL}}(q(x_N | x_0) || p_{\theta_N}(x_N)) = \mathbb{E}_{x_N \sim q(x_N | x_0)} [-\log p_\theta(x_N)] + C \approx -\log \pi_{k^*} + C, \quad (13)$$

for  $k^* = \operatorname{argmin}_k \|\mu_k - x_0\|$ . Note that we can still formulate the  $L_2$  loss in this framework with  $K = 1$  and  $\mathcal{B} = \mathcal{N}$ .

### 5.2 Refinement Losses

At the refinement stage, non-robust  $L_p$  losses [55, 14, 65] are commonly used as

$$\log p_{\theta_i}(x_i^B | x_i^A, x_{i+1}^A, x_{i+1}^B) = \|x_i^B - \mu_{\theta_i}\|_2^p + C. \quad (14)$$

Such a loss, as we argued in Section 3, leads to poor gradients when the conditioning fails, i.e., when the model is not able to approximately find the correct match. An alternative is to condition on  $q$  directly, which removes the outlier problem. However, as discussed in Section 3, this formulation struggles with distribution shifts during inference. It then is intuitive to somehow *interpolate* between these two extremes. To this end, we consider the generalized robust loss proposed by Barron [3],

$$\log p(x; \alpha, c) = \frac{|\alpha - 2|}{\alpha} \left( \left( \frac{x^2}{c^2 |\alpha - 2|} + 1 \right)^{\alpha/2} - 1 \right) + C, \quad (15)$$

<sup>1</sup>The bias is greater than reported in the paper, see this github issue.

which generalizes among others the Chabonnier [5] ( $\alpha = 0.5$ ) and Cauchy [5] ( $\lim \alpha \rightarrow 0$ ) losses.

Note that the parameter  $c$  here corresponds closely to the modeled diffusion process in Section 3. Adding in the scale  $i$  and the conditionals we get,

$$\log p_{\theta_i}(x_i^{\mathcal{B}}|x_i^{\mathcal{A}}, x_{i+1}^{\mathcal{A}}, x_{i+1}^{\mathcal{B}}, \alpha, c) = \frac{|\alpha - 2|}{\alpha} \left( \left( \frac{\|x_i^{\mathcal{B}} - \mu_{\theta_i}\|_2^2}{(ic)^2|\alpha - 2|} + 1 \right)^{\alpha/2} - 1 \right) + C, \quad (16)$$

which is the robust loss we propose to use. For all experiments, we set  $\alpha = 0.5$ , and  $c \approx 0.03$  pixels.

### 5.3 Loss Formulation

Matching networks are trained via risk minimization on a meta-dataset  $\mathcal{D}$  consisting of a large set of image pairs,

$$R(\theta) = \mathbb{E}_{(I^{\mathcal{A}}, I^{\mathcal{B}}, p(x^{\mathcal{A}}, x^{\mathcal{B}}; 0)) \sim \mathcal{D}} [\mathcal{L}(\theta; I^{\mathcal{A}}, I^{\mathcal{B}}, p)], \quad (17)$$

where

$$\mathcal{L}(\theta; I^{\mathcal{A}}, I^{\mathcal{B}}, p(x^{\mathcal{A}}, x^{\mathcal{B}}; 0)) = \mathcal{L}_{\text{Refine}}(\theta; I^{\mathcal{A}}, I^{\mathcal{B}}, p) + \mathcal{L}_{\text{Match}}(\theta; I^{\mathcal{A}}, I^{\mathcal{B}}, p). \quad (18)$$

The refinement and coarse matching losses are defined by,

$$\mathcal{L}_{\text{Refine}} = \mathbb{E}_{x_0 \sim p} \left[ \sum_{i=1}^{N-1} \mathbb{E}_{x_{i+1} \sim p_{\theta_{i+1}}} [-\log p_{\theta_i}(x_0|x_{i+1})] \right], \quad (19)$$

and

$$\mathcal{L}_{\text{Match}} = \mathbb{E}_{x_0 \sim p} \left[ D_{\text{KL}}(q(x_N|x_0) || p_{\theta_N}(x_N)) \right], \quad (20)$$

respectively. While this form includes non-robust matching, note that we use robust  $p_{\theta_N}(x_N)$  (Equation (12)) and  $p_{\theta_i}(x_0|x_{i+1})$  (Equation (16)).

## 6 Experiments

### 6.1 Training Setup

As a strong baseline, we use the training setup and network architectures as in DKM [14]. Following DKM, we use a canonical learning rate (for `batchsize = 8`) of  $10^{-4}$  for the decoder, and  $5 \cdot 10^{-6}$  for the encoder(s). We follow the same setup as in DKM for indoor and outdoor training.

### 6.2 Evaluation Metrics

We define all metrics used in the appendix.

### 6.3 Ablation Study

Here we investigate the impact of our contributions.

**Table 1: Ablation study.** We find that both the decoupled formulation and the proposed robust losses significantly increase performance.

#### Decoupled Matching and Refinement:

In Section 4 we argued for a decoupled matching process. To verify the soundness of the approach, we compare the decoupled formulation to the baseline in Table 1.

Method ↓	PCK →	@1px	@3px	@5px
Baseline		83.0	92.7	94.2
Decoupled		85.7	95.4	96.8
Decoupled + Robust Losses		<b>86.9</b>	<b>96.0</b>	<b>97.3</b>

**Robust Losses:** Given our decoupled framework, we proposed two distinctly different losses suitable for the distinct qualities of the identified subtasks. For the coarse matching stage we proposed a regression-by-classification approach, to be able to represent free-form matching distributions. In contrast, for the refinement stage, we proposed robust regression losses for sub-pixel precision. We investigate the impact of this in Table 1.

Table 2: **SotA comparison on the HPatches Homography benchmark.** Measured in AUC (higher is better).

Method ↓	AUC →	@3px	@5px	@10px
SuperGlue [41] CVPR'19		53.9	68.3	81.7
LoFTR [48] CVPR'21		65.9	75.6	84.6
3DG-STFM [34] ECCV'22		64.7	73.1	81.0
ASpanFormer [10] ECCV'22		67.4	76.9	85.6
TopicFM [19] AAAI'23		67.3	77.0	85.7
PDC-Net+ [57] TPAMI'23		67.7	77.6	86.3
DKM [14] CVPR'23		71.3	80.6	88.5
ASTR [66] CVPR'23		71.7	80.3	88.0
PMatch [67] CVPR'23		71.9	80.7	88.5
<b>RoMa</b>		<b>72.2</b>	<b>81.2</b>	<b>89.1</b>

Table 3: **SotA comparison on the Megadepth-1500 and ScanNet-1500 benchmark.** Measured in AUC (higher is better).

Method ↓	AUC →	Megadepth-1500			ScanNet-1500		
		@5°	@10°	@20°	@5°	@10°	@20°
SuperGlue [41] CVPR'19		42.2	61.2	76.0	16.2	33.8	51.8
PDC-Net [56] CVPR'21		-	-	-	18.7	37.0	54.0
LoFTR [48] CVPR'21		52.8	69.2	81.2	22.1	40.8	57.6
PDC-Net+ [57] TPAMI'23		51.5	67.2	78.5	20.3	39.4	57.1
QuadTree [50] ICLR'22		54.6	70.5	82.2	24.9	44.7	61.8
MatchFormer [60] ACCV'22		52.9	69.7	82.0	24.3	43.9	61.4
ECO-TR [49] ECCV'22		48.3	65.8	78.5	-	-	-
3DG-STFM [34] ECCV'22		52.6	68.5	80.0	23.6	43.6	61.2
ASpanFormer [10] ECCV'22		55.3	71.5	83.1	25.6	46.0	63.3
TopicFM [19] AAAI'23		54.1	70.1	81.6	-	-	-
PATS [37] CVPR'23		-	-	-	26.0	46.9	64.3
ASTR [66] CVPR'23		58.4	73.1	83.8	-	-	-
DKM [14] CVPR'23		60.4	74.9	85.1	29.4	50.7	68.3
PMatch [67] CVPR'23		61.4	75.7	85.7	29.4	50.1	67.4
<b>RoMa</b>		<b>62.6</b>	<b>76.7</b>	<b>86.3</b>	<b>31.8</b>	<b>53.4</b>	<b>70.9</b>

## 6.4 Outdoor Geometry Estimation

**HPatches Homography Estimation:** HPatches [1] depicts planar scenes divided in sequences, with transformations restricted to homographies. We follow the evaluation protocol proposed LoFTR [48]. Table 2 shows that RoMa achieves SotA performance.

**MegaDepth-1500 Pose Estimation:** We use the MegaDepth-1500 test set [48] which consists of 1500 pairs from scene 0015 (St. Peter’s Basilica) and 0022 (Brandenburger Tor). We follow the protocol in [48, 10] and use a RANSAC threshold of 0.5 with intrinsics equivalent to a longer side of 1200. Our results, presented in Table 3, show that our method sets a new state-of-the-art.

**Megadepth-8-Scenes:** We evaluate RoMa on the MegaDepth-8-scenes benchmark, introduced in DKM [14]. RoMa achieves large gains in performance, see Table 5.

**Image Matching Challenge 2022:** We achieve state-of-the-art results on the IMC2022 benchmark, with a score of 88.0 mAA@10, see Table 6 for details.

## 6.5 Indoor Geometry Estimation

**ScanNet-1500 Pose Estimation:** ScanNet [11] is a large scale indoor dataset, composed of challenging sequences with low texture regions and large changes in perspective. We follow the evaluation in SuperGlue [41]. Results are presented in Table 3. RoMa shows gains of +2.4 AUC@5° compared to the previous best method.

## 7 Conclusion

In this work, we revisited robust losses for dense matching from a novel probabilistic perspective by means of a Markov chain formulation. In this framework, we analyzed the matching process, yielding several insights. Our analysis motivated two improvements. First, we decoupled coarse matching from refinement. Second, we proposed suitable robust losses for each. These two improvements gave large improvements in performance.

### Limitations and Future Work:

- (a) While we show that our proposed robust loss formulation can substantially improve dense feature matching, there are multiple ways of defining a forward process that we have not explored. We hope that this work will inspire researchers to further explore this topic.
- (b) Our approach relies on supervised warps, which limits the amount of usable data. Investigating how to incorporate self-supervision, e.g., as in PMatch [67], is important.

**Acknowledgements:** This work was supported by the Wallenberg Artificial Intelligence, Autonomous Systems and Software Program (WASP), funded by Knut and Alice Wallenberg Foundation; and by the strategic research environment ELLIIT funded by the Swedish government. The computational resources were provided by the National Academic Infrastructure for Supercomputing in Sweden (NAISS) at C3SE partially funded by the Swedish Research Council through grant agreement no. 2022-06725, and by the Berzelius resource, provided by the Knut and Alice Wallenberg Foundation at the National Supercomputer Centre.

## References

- [1] Vassileios Balntas, Karel Lenc, Andrea Vedaldi, and Krystian Mikolajczyk. HPatches: A benchmark and evaluation of handcrafted and learned local descriptors. In *Proceedings of the IEEE conference on computer vision and pattern recognition*, pages 5173–5182, 2017.
- [2] Daniel Barath, Jana Noskova, Maksym Ivashechkin, and Jiri Matas. Magsac++, a fast, reliable and accurate robust estimator. In *Proceedings of the IEEE/CVF conference on computer vision and pattern recognition*, pages 1304–1312, 2020.
- [3] Jonathan T Barron. A general and adaptive robust loss function. In *Proceedings of the IEEE/CVF Conference on Computer Vision and Pattern Recognition*, pages 4331–4339, 2019.
- [4] Herbert Bay, Tinne Tuytelaars, and Luc Van Gool. Surf: Speeded up robust features. In *European conference on computer vision*, pages 404–417. Springer, 2006.
- [5] Michael J Black and Paul Anandan. The robust estimation of multiple motions: Parametric and piecewise-smooth flow fields. *Computer vision and image understanding*, 63(1):75–104, 1996.
- [6] Michael J Black and Anand Rangarajan. On the unification of line processes, outlier rejection, and robust statistics with applications in early vision. *International journal of computer vision*, 19(1):57–91, 1996.
- [7] Georg Bökman and Fredrik Kahl. A case for using rotation invariant features in state of the art feature matchers. In *Proceedings of the IEEE/CVF Conference on Computer Vision and Pattern Recognition*, pages 5110–5119, 2022.
- [8] Leo Breiman, JH Friedman, RA Olshen, and CJ Stone. Classification and regression trees. wadsworth & brooks. *Cole Statistics/Probability Series*, 1984.
- [9] Ignas Budvytis, Marvin Teichmann, Tomas Vojir, and Roberto Cipolla. Large scale joint semantic re-localisation and scene understanding via globally unique instance coordinate regression. In Kirill Sidorov and Yulia Hicks, editors, *Proceedings of the British Machine Vision Conference (BMVC)*, pages 86.1–86.13. BMVA Press, September 2019. doi: 10.5244/C.33.86. URL <https://dx.doi.org/10.5244/C.33.86>.
- [10] Hongkai Chen, Zixin Luo, Lei Zhou, Yurun Tian, Mingmin Zhen, Tian Fang, David Mckinnon, Yanghai Tsin, and Long Quan. ASpanFormer: Detector-free image matching with adaptive span transformer. In *Proc. European Conference on Computer Vision (ECCV)*, 2022.
- [11] Angela Dai, Angel X Chang, Manolis Savva, Maciej Halber, Thomas Funkhouser, and Matthias Nießner. Scannet: Richly-annotated 3d reconstructions of indoor scenes. In *Proceedings of the IEEE conference on computer vision and pattern recognition*, pages 5828–5839, 2017.

- [12] Daniel DeTone, Tomasz Malisiewicz, and Andrew Rabinovich. Superpoint: Self-supervised interest point detection and description. In *Proceedings of the IEEE conference on computer vision and pattern recognition workshops*, pages 224–236, 2018.
- [13] Alexey Dosovitskiy, Lucas Beyer, Alexander Kolesnikov, Dirk Weissenborn, Xiaohua Zhai, Thomas Unterthiner, Mostafa Dehghani, Matthias Minderer, Georg Heigold, Sylvain Gelly, Jakob Uszkoreit, and Neil Houlsby. An image is worth 16x16 words: Transformers for image recognition at scale. In *International Conference on Learning Representations*, 2021. URL <https://openreview.net/forum?id=YicbFdNTTy>.
- [14] Johan Edstedt, Ioannis Athanasiadis, Mårten Wadenbäck, and Michael Felsberg. DKM: Dense kernelized feature matching for geometry estimation. In *IEEE Conference on Computer Vision and Pattern Recognition*, 2023.
- [15] Michael Felsberg, P-E Forssen, and H Schar. Channel smoothing: Efficient robust smoothing of low-level signal features. *IEEE Transactions on Pattern Analysis and Machine Intelligence*, 28(2):209–222, 2006.
- [16] Divyansh Garg, Yan Wang, Bharath Hariharan, Mark Campbell, Kilian Q Weinberger, and Wei-Lun Chao. Wasserstein distances for stereo disparity estimation. *Advances in Neural Information Processing Systems*, 33:22517–22529, 2020.
- [17] Robert Geirhos, Patricia Rubisch, Claudio Michaelis, Matthias Bethge, Felix A. Wichmann, and Wieland Brendel. Imagenet-trained CNNs are biased towards texture; increasing shape bias improves accuracy and robustness. In *International Conference on Learning Representations*, 2019. URL <https://openreview.net/forum?id=Bygh9j09KX>.
- [18] Robert Geirhos, Kantharaju Narayanappa, Benjamin Mitzkus, Tizian Thieringer, Matthias Bethge, Felix A Wichmann, and Wieland Brendel. Partial success in closing the gap between human and machine vision. *Advances in Neural Information Processing Systems*, 34:23885–23899, 2021.
- [19] Khang Truong Giang, Soohwan Song, and Sungho Jo. TopicFM: Robust and interpretable topic-assisted feature matching. In *Proceedings of the AAAI Conference on Artificial Intelligence*, volume 37, 2023.
- [20] Gustav Häger, Mikael Persson, and Michael Felsberg. Predicting disparity distributions. In *2021 IEEE International Conference on Robotics and Automation (ICRA)*, pages 4363–4369. IEEE, 2021.
- [21] Stephen Hausler, Sourav Garg, Ming Xu, Michael Milford, and Tobias Fischer. Patch-netvlad: Multi-scale fusion of locally-global descriptors for place recognition. In *Proceedings of the IEEE/CVF Conference on Computer Vision and Pattern Recognition*, pages 14141–14152, 2021.
- [22] Kaiming He, Xinlei Chen, Saining Xie, Yanghao Li, Piotr Dollár, and Ross Girshick. Masked autoencoders are scalable vision learners. In *Proceedings of the IEEE/CVF Conference on Computer Vision and Pattern Recognition (CVPR)*, pages 16000–16009, June 2022.
- [23] Jonathan Ho, Ajay Jain, and Pieter Abbeel. Denoising diffusion probabilistic models. *Advances in Neural Information Processing Systems*, 33:6840–6851, 2020.
- [24] Addison Howard, Eduard Trulls, etru1927, Kwang Moo Yi, old ufo, Sohler Dane, and Yuhe Jin. Image matching challenge 2022, 2022. URL <https://kaggle.com/competitions/image-matching-challenge-2022>.
- [25] Aapo Hyvärinen and Peter Dayan. Estimation of non-normalized statistical models by score matching. *Journal of Machine Learning Research*, 6(4), 2005.
- [26] Wei Jiang, Eduard Trulls, Jan Hosang, Andrea Tagliasacchi, and Kwang Moo Yi. COTR: Correspondence Transformer for Matching Across Images. In *ICCV*, 2021.
- [27] Tero Karras, Miika Aittala, Timo Aila, and Samuli Laine. Elucidating the design space of diffusion-based generative models. In Alice H. Oh, Alekh Agarwal, Danielle Belgrave, and Kyunghyun Cho, editors, *Advances in Neural Information Processing Systems*, 2022. URL <https://openreview.net/forum?id=k7FuTOWM0c7>.
- [28] Jan J Koenderink. The structure of images. *Biological cybernetics*, 50(5):363–370, 1984.
- [29] Xiaotian Li, Shuzhe Wang, Yi Zhao, Jakob Verbeek, and Juho Kannala. Hierarchical scene coordinate classification and regression for visual localization. In *Proceedings of the IEEE/CVF Conference on Computer Vision and Pattern Recognition*, pages 11983–11992, 2020.

- [30] Tony Lindeberg. Scale-space theory: A basic tool for analyzing structures at different scales. *Journal of applied statistics*, 21(1-2):225–270, 1994.
- [31] Philipp Lindenberger, Paul-Edouard Sarlin, Viktor Larsson, and Marc Pollefeys. Pixel-perfect structure-from-motion with featuremetric refinement. In *Proceedings of the IEEE/CVF International Conference on Computer Vision*, pages 5987–5997, 2021.
- [32] Haisong Liu, Tao Lu, Yihui Xu, Jia Liu, Wenjie Li, and Lijun Chen. Camliflow: bidirectional camera-lidar fusion for joint optical flow and scene flow estimation. In *Proceedings of the IEEE/CVF Conference on Computer Vision and Pattern Recognition*, pages 5791–5801, 2022.
- [33] David G Lowe. Distinctive image features from scale-invariant keypoints. *International journal of computer vision*, 60(2):91–110, 2004.
- [34] Runyu Mao, Chen Bai, Yatong An, Fengqing Zhu, and Cheng Lu. 3DG-STFM: 3d geometric guided student-teacher feature matching. In *Proc. European Conference on Computer Vision (ECCV)*, 2022.
- [35] Iaroslav Melekhov, Aleksei Tiulpin, Torsten Sattler, Marc Pollefeys, Esa Rahtu, and Juho Kannala. Dgc-net: Dense geometric correspondence network. In *2019 IEEE Winter Conference on Applications of Computer Vision (WACV)*, pages 1034–1042. IEEE, 2019.
- [36] Muhammad Muzammal Naseer, Kanchana Ranasinghe, Salman H Khan, Munawar Hayat, Fahad Shahbaz Khan, and Ming-Hsuan Yang. Intriguing properties of vision transformers. *NeurIPS*, 34:23296–23308, 2021.
- [37] Junjie Ni, Yijin Li, Zhaoyang Huang, Hongsheng Li, Hujun Bao, Zhaopeng Cui, and Guofeng Zhang. Pats: Patch area transportation with subdivision for local feature matching. In *The IEEE/CVF Computer Vision and Pattern Recognition Conference (CVPR)*, 2023.
- [38] Maxime Oquab, Timothée Darcet, Theo Moutakanni, Huy V. Vo, Marc Szafraniec, Vasil Khalidov, Pierre Fernandez, Daniel Haziza, Francisco Massa, Alaaeldin El-Nouby, Russell Howes, Po-Yao Huang, Hu Xu, Vasu Sharma, Shang-Wen Li, Wojciech Galuba, Mike Rabbat, Mido Assran, Nicolas Ballas, Gabriel Synnaeve, Ishan Misra, Herve Jegou, Julien Mairal, Patrick Labatut, Armand Joulin, and Piotr Bojanowski. DINOv2: Learning robust visual features without supervision. *arXiv:2304.07193*, 2023.
- [39] John R Quinlan et al. Learning with continuous classes. In *5th Australian joint conference on artificial intelligence*, volume 92, pages 343–348. World Scientific, 1992.
- [40] Jerome Revaud, Cesar De Souza, Martin Humenberger, and Philippe Weinzaepfel. R2d2: Reliable and repeatable detector and descriptor. *Advances in neural information processing systems*, 32:12405–12415, 2019.
- [41] Paul-Edouard Sarlin, Daniel DeTone, Tomasz Malisiewicz, and Andrew Rabinovich. Superglue: Learning feature matching with graph neural networks. In *Proceedings of the IEEE/CVF conference on computer vision and pattern recognition*, pages 4938–4947, 2020.
- [42] Paul-Edouard Sarlin, Ajaykumar Unagar, Mans Larsson, Hugo Germain, Carl Toft, Viktor Larsson, Marc Pollefeys, Vincent Lepetit, Lars Hammarstrand, Fredrik Kahl, et al. Back to the feature: Learning robust camera localization from pixels to pose. In *Proceedings of the IEEE/CVF conference on computer vision and pattern recognition*, pages 3247–3257, 2021.
- [43] Johannes L Schonberger and Jan-Michael Frahm. Structure-from-motion revisited. In *Proceedings of the IEEE conference on computer vision and pattern recognition*, pages 4104–4113, 2016.
- [44] Karen Simonyan and Andrew Zisserman. Very deep convolutional networks for large-scale image recognition. In *3rd International Conference on Learning Representations, ICLR 2015, San Diego, CA, USA, May 7-9, 2015, Conference Track Proceedings*, 2015.
- [45] Jascha Sohl-Dickstein, Eric Weiss, Niru Maheswaranathan, and Surya Ganguli. Deep unsupervised learning using nonequilibrium thermodynamics. In Francis Bach and David Blei, editors, *Proceedings of the 32nd International Conference on Machine Learning*, volume 37 of *Proceedings of Machine Learning Research*, pages 2256–2265, Lille, France, 07–09 Jul 2015. PMLR. URL <https://proceedings.mlr.press/v37/sohl-dickstein15.html>.
- [46] Yang Song and Stefano Ermon. Generative modeling by estimating gradients of the data distribution. *Advances in neural information processing systems*, 32, 2019.

- [47] Yang Song, Jascha Sohl-Dickstein, Diederik P Kingma, Abhishek Kumar, Stefano Ermon, and Ben Poole. Score-based generative modeling through stochastic differential equations. In *International Conference on Learning Representations*, 2021. URL <https://openreview.net/forum?id=PxtIG12RRHS>.
- [48] Jiaming Sun, Zehong Shen, Yuang Wang, Hujun Bao, and Xiaowei Zhou. LoFTR: Detector-free local feature matching with transformers. In *Proceedings of the IEEE/CVF Conference on Computer Vision and Pattern Recognition*, pages 8922–8931, 2021.
- [49] Dongli Tan, Jiang-Jiang Liu, Xingyu Chen, Chao Chen, Ruixin Zhang, Yunhang Shen, Shouhong Ding, and Rongrong Ji. ECO-TR: Efficient Correspondences Finding Via Coarse-to-Fine Refinement. In *Proc. European Conference on Computer Vision (ECCV)*, 2022.
- [50] Shitao Tang, Jiahui Zhang, Siyu Zhu, and Ping Tan. Quadtree attention for vision transformers. In *International Conference on Learning Representations*, 2022. URL [https://openreview.net/forum?id=fR-EnKWL\\_Zb](https://openreview.net/forum?id=fR-EnKWL_Zb).
- [51] Luís Torgo and João Gama. Regression by classification. In Dábio L. Borges and Celso A. A. Kaestner, editors, *Advances in Artificial Intelligence*, pages 51–60, Berlin, Heidelberg, 1996. Springer Berlin Heidelberg. ISBN 978-3-540-70742-4.
- [52] Philip HS Torr and David W Murray. Outlier detection and motion segmentation. In *Sensor Fusion VI*, volume 2059, pages 432–443. SPIE, 1993.
- [53] Philip HS Torr and David William Murray. The development and comparison of robust methods for estimating the fundamental matrix. *International journal of computer vision*, 24:271–300, 1997.
- [54] Prune Truong, Martin Danelljan, Luc V Gool, and Radu Timofte. GOCor: Bringing Globally Optimized Correspondence Volumes into Your Neural Network. *Advances in Neural Information Processing Systems*, 33, 2020.
- [55] Prune Truong, Martin Danelljan, and Radu Timofte. GLU-Net: Global-local universal network for dense flow and correspondences. In *Proceedings of the IEEE/CVF conference on computer vision and pattern recognition*, pages 6258–6268, 2020.
- [56] Prune Truong, Martin Danelljan, Luc Van Gool, and Radu Timofte. Learning accurate dense correspondences and when to trust them. In *Proceedings of the IEEE/CVF Conference on Computer Vision and Pattern Recognition*, pages 5714–5724, 2021.
- [57] Prune Truong, Martin Danelljan, Radu Timofte, and Luc Van Gool. PDC-Net+: Enhanced Probabilistic Dense Correspondence Network. *IEEE Transactions on Pattern Analysis and Machine Intelligence*, 2023.
- [58] Michal J. Tyszkiewicz, Pascal Fua, and Eduard Trulls. DISK: learning local features with policy gradient. In *NeurIPS*, 2020.
- [59] Pascal Vincent. A connection between score matching and denoising autoencoders. *Neural computation*, 23(7):1661–1674, 2011.
- [60] Qing Wang, Jiaming Zhang, Kailun Yang, Kunyu Peng, and Rainer Stiefelhagen. MatchFormer: Interleaving attention in transformers for feature matching. In *Asian Conference on Computer Vision*, 2022.
- [61] Chen Wei, Haoqi Fan, Saining Xie, Chao-Yuan Wu, Alan Yuille, and Christoph Feichtenhofer. Masked feature prediction for self-supervised visual pre-training. In *Proceedings of the IEEE/CVF Conference on Computer Vision and Pattern Recognition*, pages 14668–14678, 2022.
- [62] Sholom M. Weiss and Nitin Indurkha. Rule-based regression. In Ruzena Bajcsy, editor, *Proceedings of the 13th International Joint Conference on Artificial Intelligence. Chambéry, France, August 28 - September 3, 1993*, pages 1072–1078. Morgan Kaufmann, 1993.
- [63] Sholom M. Weiss and Nitin Indurkha. Rule-based machine learning methods for functional prediction. *J. Artif. Intell. Res.*, 3:383–403, 1995. doi: 10.1613/jair.199. URL <https://doi.org/10.1613/jair.199>.
- [64] Andrew P. Witkin. Scale space filtering. *Proc. 8th International Joint on Artificial Intelligence*, pages 1091–1022, 1983.
- [65] Haofei Xu, Jing Zhang, Jianfei Cai, Hamid Rezaatofighi, and Dacheng Tao. Gmflow: Learning optical flow via global matching. *Proceedings of the IEEE/CVF Conference on Computer Vision and Pattern Recognition*, 2022.

- [66] Jiahuan Yu, Jiahao Chang, Jianfeng He, Tianzhu Zhang, Jiyang Yu, and Wu Feng. ASTR: Adaptive spot-guided transformer for consistent local feature matching. In *The IEEE/CVF Computer Vision and Pattern Recognition Conference (CVPR)*, 2023.
- [67] Shengjie Zhu and Xiaoming Liu. PMatch: Paired masked image modeling for dense geometric matching. In *Proceedings of the IEEE/CVF Conference on Computer Vision and Pattern Recognition*, 2023.

## Appendix

### A Dataset Licenses

In Table 4 we provide the licenses of the datasets used in the paper.

Table 4: **Table of dataset licenses.**

Dataset	License
MegaDepth	MIT
ScanNet	Non-Commercial
HPatches	MIT

### B Additional Benchmarks

**MegaDepth-8-Scenes:** Here we compare RoMa to the state-of-the-art on the Megadepth-8-Scenes benchmark, introduced in DKM [14]. We show results in Table 5. RoMa achieves gains of  $+1.7\text{AUC}@5^\circ$  compared to the previous best result.

Table 5: Pose estimation results on the Megadepth-8-Scenes benchmark, measured in AUC (higher is better).

Method ↓	AUC →	@5°	@10°	@20°
PDCNet+ [57] <small>TPAMI'23</small>		51.8	66.6	77.2
ASpanFormer [10] <small>ECCV'22</small>		57.2	72.1	82.9
DKM [14] <small>CVPR'23</small>		60.5	74.5	84.2
<b>RoMa</b>		<b>62.2</b>	<b>75.9</b>	<b>85.3</b>

**Image Matching Challenge 2022:** We submit to the 2022 version of the image matching challenge [24], which consists of a hidden test-set of Google street-view images with the task to estimate the fundamental matrix between them. Given a fundamental matrix, the error is computed in terms of rotation ( $\epsilon_R$  in degrees) and translation ( $\epsilon_T$  in meters). Given one threshold over each, the pose is classified as accurate if it meets both thresholds. In code:

```
thresholds_r = np.linspace(1, 10, 10) # In degrees.
thresholds_t = np.geomspace(0.2, 5, 10) # In meters.
```

The percentage of image pairs that meet every pair of thresholds is computed, the results are averaged over all thresholds, which rewards more accurate poses. As the dataset contains multiple scenes, which may have a different number of pairs, the metric is computed separately for each scene and then averaged. We refer to this metric as mAA@10. We present results in Table 6. We significantly outperform the state-of-the-art with a score of 88.0, a gain of  $+4.2\text{mAA}@10$  compared to the previous best.

### C Additional Qualitative Examples

In Figure 5 and Figure 6 we qualitatively illustrate the robustness of RoMa to extreme changes in viewpoint. RoMa is robust to large changes in 3D perspectives, including scale, rotation, and skew.



Figure 5: **Qualitative Illustration of Extreme Viewpoint Robustness.** We illustrate RoMa's robustness to viewpoint changes.



Figure 6: **Qualitative Illustration of Extreme Viewpoint Robustness.** We illustrate RoMa's robustness to viewpoint changes.

Table 6: Relative pose estimation results on IMC2022 [24], measured in mAA (higher is better). Performance for previous methods taken from [10]

Method ↓	mAA →	@10
SP [12]+SuperGlue [41]		72.4
LoFTR [48]		78.3
MatchFormer [60]		78.3
QuadTree [50]		81.7
ASpanFormer [10]		83.8
<b>RoMa</b>		<b>88.0</b>

## D Definitions of Evaluation Metrics

**AUC:** We use the Area Under the Curve (AUC) to evaluate performance. We define the  $AUC@t$  as the integral of the precision up to the threshold  $t$ . In practice, this is approximated using the trapezoidal rule, as in previous work [14, 57, 48].

**PCK:** We use the Percent Correct Keypoints (PCK) metric to evaluate the accuracy of the dense warp. This metric measures the warp precision at some threshold  $t$ . We use  $t = 1, 3, 5$  pixels in the paper.

**Precision:** For relative pose estimation, the precision is defined as

$$\text{RelPosePrecision}@t = \max(|\varepsilon_{\hat{t}}, |\varepsilon_{\hat{R}}|) < t \quad (21)$$

where

$$\varepsilon_{\hat{t}} = \cos \frac{\langle t, \hat{t} \rangle}{\|t\| \cdot \|\hat{t}\|} \quad (22)$$

and

$$\varepsilon_{\hat{R}} = \arccos \left( (\text{tr}(\hat{R}^T R) - 1) / 2 \right) \quad (23)$$

For homography estimation the precision is defined as

$$\text{HomographyPrecision}@t = \frac{1}{4} \sum_{x_i \in \text{image corners}} \|\hat{H}(x_i) - H(x_i)\|_2 < t, \quad (24)$$

i.e., that the average distance between image corners transformed by the estimated homography and the true homography is under some pixel threshold  $t$ .

For dense warp evaluation (as in the ablation study) the precision is defined as

$$\text{WarpPrecision}@t = \frac{1}{|\text{matchable pixels}|} \sum_{x \in \text{matchable pixels}} \|\hat{W}(x) - W(x)\|_2 < t, \quad (25)$$

## E Architecture of Proposed Coarse Decoder

The proposed coarse Transformer decoder consists of 5 ViT blocks, with 8 heads, hidden size D 1024, and MLP size 4096. The input is the concatenation of projected DINOv2 [38] features (of dimension 512) and the output of the GP module proposed in DKM [14] (of dimension 512). The output is a vector of  $B \times H \times W \times K + 1$  where  $K$  is the number of classification anchors (parameterizing the conditional distribution), and 1 is the matchability score (marginal distribution).

## F Additional Training and Evaluation Details

**Resolution:** RoMa is trained on a fixed resolution of  $560 \times 560$ . During inference, the resolution is set to  $672 \times 672$ , and the predictions are upsampled using the refiners like previous work [57, 14]. We use an upsampling resolution of  $1344 \times 1344$ . For the ablation study we used a slightly lower resolution of  $448 \times 448$ .

**Compute:** Training RoMa takes 4 days on 4 A100 GPUs. For lower resolution models ( $448 \times 448$ ), training takes 2.5 days.